

Experimental Determination of the Energy Distribution Functions and Analysis of the Energy-Loss Mechanisms of Hot Carriers in *p*-Type Germanium*

WILLIAM E. PINSON† AND RALPH BRAY

Department of Physics, Purdue University, Lafayette, Indiana

(Received 6 July 1964)

This paper contains a description of an experimental determination of the energy distribution functions of hot holes in germanium, and the application of the results to the analysis of the dominant scattering and energy-loss mechanisms. The distribution functions are obtained from the study of the modulation of the free-hole, intervalence-band absorption of infrared radiation by application of pulses of high electric field. Details of the distribution function can be obtained because a correlation exists between the absorption at a given wavelength and the hole concentration at a given energy. An auxiliary investigation of the temperature dependence of the equilibrium absorption spectrum empirically supplies the necessary calibrating relations for the above correlation and an approximate valence-band structure with equivalent spherical energy surfaces. The hot-carrier studies were made at field strengths up to 2800 V/cm, at 77°K, on germanium samples with hole concentrations in the range of $10^{15}/\text{cm}^3$. The infrared modulation effects are themselves of interest and the techniques are described in detail. Positive and negative modulation of transmitted intensity as high as 50% could be obtained. The dependence of the modulation (and distribution functions) on crystallographic direction, carrier concentration, and polarization of the light was investigated. Three features of the experimental distributions stand out: (a) the non-Maxwellian character, typified by the relatively small number of high-energy carriers, (b) the slow rise in average energy from 0.01 to 0.028 eV as the field strength is raised to 2000 V/cm, and (c) the large ratios of drift to root-mean-square velocity, $v_d/v_{\text{rms}} \gtrsim 0.4$ for $E > 400$ V/cm, corresponding to strong displacement of the hole distributions in momentum space. These features, together with energy-loss rate calculations, substantiate the importance of inelastic scattering and the dominant role of optical-phonon interactions. A picture of the steady-state hot-carrier effect emerges, emphasizing a cyclic streaming motion of holes in \mathbf{k} space, in contrast to the usual diffusion formulation. Briefly indicated are some consequences of this picture regarding the relative population of light and heavy holes, the anisotropy of infrared absorption and hot-carrier mobility, and the efficiency of impact ionization of deep-lying acceptors.

I. INTRODUCTION

THE general objectives of the present work are (1) to determine experimentally the energy distribution function of hot carriers in *p*-type germanium, and (2) to apply the results to analyze the role of the prevalent scattering and energy-loss mechanisms of the carriers. The distribution functions are obtained from the study of the modulation of the free hole, intervalence band absorption of infrared radiation by application of short pulses of high electric field.¹⁻⁵ The latter alter the distribution function of the free holes, without appreci-

ably changing their concentration or the lattice temperature.⁶

The present approach to the study of the properties of hot carriers represents a departure from the usual one of studying the field dependence of the mobility. Although the hot-carrier mobility can be measured readily, it can not be analyzed without many simplifying assumptions in the description of the band structure, the scattering mechanisms, and particularly in the theoretical derivation of the distribution function. Recognition of the difficulties inherent in the analysis of the mobility has motivated some recent attempts to determine experimentally more fundamental properties of hot carriers, e.g., the distribution function itself, or at least the average energy or effective temperature of the hot carriers. Approaches have been reported based on measurements of the noise of hot carriers,⁷ and also of their thermoelectric power.⁸ In both these cases, only average properties of the hot carriers can be obtained, from which an effective temperature may be estimated. However, in the method under consideration here, involving

* Work supported in part by the U. S. Army Research Office and the Advanced Research Projects Agency.

† Present address: National Cash Register, London, England.

¹ The observation of hot-carrier modulation of the intervalence band absorption spectrum in germanium, and its possible application to the analysis of the properties of hot carriers were reported independently by R. Bray and E. G. S. Paige in the discussion following the paper by R. Bray and D. M. Brown, Ref. 15, p. 105. Initial results, at field strengths below 350 V/cm and temperatures between 93 and 297°K, were reported by M. A. C. S. Brown *et al.* (Refs. 2 and 3). An account of most of the work to be presented here, at field strengths up to 2800 V/cm, at 77°K, was given in Bull. Am. Phys. Soc. 8, 253 (1963) in two papers by the present authors. A summary of most of the present findings, as well as an extension to novel aspects is given in Ref. 4, and a similar account is contained in Ref. 5.

² M. A. C. S. Brown and E. G. S. Paige, Phys. Rev. Letters 7, 84 (1961).

³ M. A. C. S. Brown, E. G. S. Paige, and L. N. Simcox, *Proceedings of the International Conference on the Physics of Semiconductors, Exeter, 1962* (The Institute of Physics and the Physical Society, London, 1962), p. 111.

⁴ R. Bray and W. Pinson, Phys. Rev. Letters 11, 268 (1963).

⁵ A. C. Baynham and E. G. S. Paige, Phys. Letters 6, 7 (1963).

⁶ For review articles and early references on hot carriers, see J. B. Gunn, *Progress in Semiconductors* (John Wiley & Sons, Inc., New York, 1957), Vol. 2, p. 213; and S. H. Koenig, Phys. Chem. Solids 8, 227 (1959).

⁷ E. Erlbach and J. B. Gunn, Phys. Rev. Letters 8, 280 (1962); also, *Proceedings of the International Conference on Physics of Semiconductors, Exeter, 1962* (The Institute of Physics and the Physical Society, London, 1962), p. 128.

⁸ J. K. Pozhela, V. K. Repshas, and V. J. Shilalnikas, *Proceedings of the International Conference on Physics of Semiconductors, Exeter, 1962*, (The Institute of Physics and the Physical Society, London, 1962), p. 149; J. Zucker, Bull. Am. Phys. Soc. 9, 62 (1964).

the study of the intervalence-band absorption spectrum of hot carriers in *p*-type germanium, it is possible to obtain *details* of the distribution function of hot carriers, because a correlation exists between the absorption at a given wavelength and the hole concentration at a given energy. This property is a consequence of the fact that intervalence band transitions are direct.

A brief review of the various theoretical approaches to the determination of the hot-carrier distribution function provides some specific objectives for the experimental study. The simplest form for a hot-carrier distribution is a displaced Maxwellian distribution, characterized by a carrier temperature greater than the lattice temperature. This form is valid if carrier-carrier scattering is so strong that both energy and momentum interchange between carriers are dominant over all other carrier interactions. If the energy but not the momentum interchange between carriers is dominant, then only the isotropic part of the distribution function may be taken to be Maxwellian. These considerations were introduced by Fröhlich.⁹ Because of the simplicity of such an approach, the Maxwellian distribution has been applied very widely, usually without regard to its validity in particular cases. When sufficiently strong carrier-carrier scattering can not be assumed, it is necessary to derive the form of the distribution function from solution of the Boltzmann transport equation. In this case the strength of the various scattering mechanisms must be specified, and naturally the results will depend on what assumptions are made. The abundance of literature on this subject attests to the variety of the possibilities.^{6,10} The major point of interest to us is the fact that *nearly all theoretical formulations are based on the diffusion approximation*, in which the hot-carrier distribution is assumed to be nearly isotropic, and adequately represented by the first two terms (P_0 and P_1) in the expansion of the distribution in Legendre polynomials. To put this more physically, it simply means that the ratio of drift to random velocity is taken to be much smaller than unity even for hot carriers. Only recently has there been any consideration of more anisotropic distributions and higher terms in the expansion.¹¹ Such considerations have been limited to the very high-field case, when the carriers are sufficiently energetic to produce intrinsic ionization.

The experiments and analyses presented here show that the hot carrier distribution functions in *p*-type germanium are *not* Maxwellian. The most interesting

finding is that the isotropic or diffusion approximation is already invalid at relatively low-field strengths, of the order of a few hundred V/cm at 77°K, at least in *p*-type germanium.⁴ These results will be related to the important role of inelastic scattering by optical phonons.

The specific stimulus for the present work came from earlier studies of the mobility in *p*-type germanium. An important role had been attributed to the interaction of optical phonons with holes in germanium to explain the observed $T^{-2.3}$ temperature dependence of the mobility at $T \geq 100^\circ\text{K}$.¹²⁻¹⁵ However, the inclusion of this interaction in calculations of the hot-carrier mobility of holes failed to give satisfactory agreement with experiment.^{13,15} A simple hot-carrier theory was used in which the isotropic part of the distribution function was assumed to be Maxwellian, and the carrier temperature was calculated from the usual energy balance equations. It was found that the carrier temperature deduced from the analysis was much more sensitive than the calculated mobility to estimates of the strength of the optical phonon interaction. Thus it became clear that even a crude measurement of an effective hot-carrier temperature would be a most valuable analytical tool for gauging the importance of optical phonon interactions.¹⁵ The method of hot-carrier modulation of the intervalence band absorption of infrared radiation was developed with the minimal objective of measuring an effective hot-carrier temperature, but it eventually yielded much more—a rather detailed description of the hot-carrier distribution function, as well as a verification of the important role of optical phonon scattering.

It is interesting to note that while complications in the valence band structure have discouraged as extensive transport analyses in *p*-type germanium as have been made for *n*-type material, it is just this complexity that makes it uniquely possible to measure the distribution function, and to obtain interesting and quite unexpected properties of hot carriers. The blessings are mixed however; the complexity of the band structure exceeds that necessary for the success of the method, and auxiliary studies of the band structure were required to determine what approximations in the analysis were permissible.

The scheme for probing the distribution function, and analyzing the valence band structure will be described in Sec. II. This scheme requires the measurement of the pulse change in intensity of infrared radiation transmitted through *p*-type germanium, when a pulsed electric field is applied to the material. The techniques are discussed in Sec. III, which also contains the results, such as the dependence of the modulation of the absorp-

⁹ H. Fröhlich, Proc. Roy. Soc. (London) **A188**, 521, 532 (1947); H. Fröhlich and B. V. Paranjape, Proc. Phys. Soc. (London) **B69**, 21, 866 (1956). For a useful summary and further discussions, see: R. Stratton, Proc. Roy. Soc. (London) **A242**, 355 (1957).

¹⁰ A. Hasegawa and J. Yamashita, J. Phys. Soc. Japan **17**, 1751 (1962); H. G. Reik and H. Risken, Phys. Rev. **124**, 777 (1961); I. M. Dykman and P. M. Tomchuk, Fiz. Tverd. Tela **2**, 2228 (1960) [English transl.: Soviet Phys.—Solid State **2**, 1988 (1961)]; I. Adawi, Phys. Rev. **120**, 118 (1960); **115**, 1152 (1959); **112**, 1567 (1958); J. Yamashita and K. Inoue, Phys. Chem. Solids, **12**, 1 (1959); T. N. Morgan, *ibid.* **8**, 245 (1959).

¹¹ G. A. Baraff, Phys. Rev. **128**, 2507 (1962); **133**, A26 (1964).

¹² H. Ehrenreich and A. W. Overhauser, Phys. Rev. **104**, 331, 649 (1956); G. L. Bir and G. E. Pikus, Fiz. Tverd. Tela **2**, 2287 (1960) [English transl.: Soviet Phys.—Solid State **2**, 2039 (1961)].

¹³ E. M. Conwell, Phys. Chem. Solids **8**, 234 (1959).

¹⁴ D. M. Brown and R. Bray, Phys. Rev. **127**, 1593 (1962).

¹⁵ R. Bray and D. M. Brown, *International Conference on Semiconductor Physics, Prague, 1960* (Czechoslovakian Academy of Science, Prague, 1961), p. 82.

tion spectrum on field strength, E for $E \leq 2800$ V/cm, crystallographic orientation, carrier concentration, and polarization of the light. Section IV contains the experimental details and results of a subsidiary but essential measurement of the temperature dependence of the equilibrium free hole absorption spectrum. These results are required for analysis of the valence band structure, and translation of the hot carrier absorption data into distribution functions. The analysis of the hot carrier distribution function is developed in three stages of increasing complexity. In the first stage, described in Sec. V, it is determined that the hot-carrier distribution is not Maxwellian; however, estimates of average effective temperatures are made. In the second stage, the energy distribution functions themselves are determined. The latter are described in Sec. VII, while a prerequisite analysis of the valence band structure is given in Sec. VI. Also in Sec. VII, application is made of the experimentally determined energy distribution functions to determine the field dependence of (a) the average energy, (b) the ratio of drift to root-mean-square velocity of the carriers, and (c) the energy loss rate to optical and acoustical phonons. From these analyses there emerges a new and unexpected description of the hot holes, given in Sec. VIII, which emphasizes their streaming character, in contrast to the usual diffusion formulation. A third stage of analysis, consisting of a description of details of the anisotropy of the distribution in momentum space, will be described elsewhere. Brief accounts of the latter have already been published.^{4,5}

II. SCHEME FOR PROBING THE DISTRIBUTION OF HOT CARRIERS

The scheme to be discussed in this section is based on the model of the free carrier, intervalence-band absorption of infrared radiation in *p*-type germanium. We shall first review briefly its essential features as developed by Kahn¹⁶ and extended by Kane.¹⁷ The observed band character of the absorption spectrum in the 2–10 μ range is determined by three factors: the shape of the valence bands, the nature of the absorption process, and the distribution of the free holes.

The most complete description of the valence band structure near $k=0$ has been given by Kane¹⁷ from a theoretical analysis based on cyclotron resonance parameters. The "top" of the valence band consists of the heavy and light hole bands (1 and 2) touching at $k=0$. A third band is separated by 0.29 eV at $k=0$ from the two upper bands by spin-orbit interaction. According to Kane's study, band 1 may be taken to be parabolic; in band 2 the effective mass increases with energy, while in band 3 it decreases with energy. These features are incorporated in Fig. 1, where the energy of holes is plotted against k^2 . The energy surfaces in the bands are

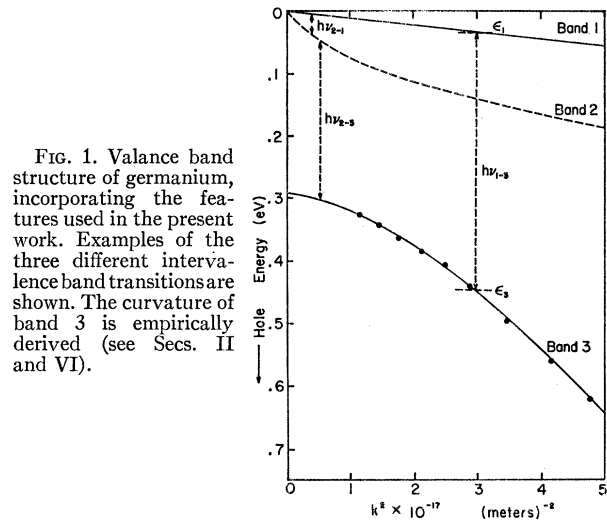


FIG. 1. Valence band structure of germanium, incorporating the features used in the present work. Examples of the three different intervalence band transitions are shown. The curvature of band 3 is empirically derived (see Secs. II and VI).

more or less warped and the structure should depend on the direction in k space, a feature not shown in Fig. 1. The structure shown in Fig. 1, is based on an average effective mass ratio of 0.35 for heavy holes in band 1, and of 0.04 for light holes near $k=0$ in band 2. Band 3 was obtained from an empirical analysis in the course of the present work, as described later in this section.

The dominant absorption process consists of direct optical transitions between the valence bands.^{16,17} Direct transitions are forbidden at $k=0$, but at $k>0$ the selection rule breaks down and such transitions can occur. Examples of the three different intervalence band transitions are shown in Fig. 1. Because of the different curvature of the three bands, and because the transitions are vertical, the three intervalence band spectra occur in different wavelength ranges. The absorption spectra of the heavy and light holes can be studied separately, from the 1–3 and 2–3 transitions respectively; all further discussions are restricted to these two absorption bands, in the range $1.8 < \lambda < 5.0 \mu$.¹⁸

The absorption due to holes in a volume element in k space, depends on the number of holes available in the given band to make the vertical transition to another band at higher hole energy. Thus the absorption spectra depend strongly on the distribution functions of the holes.^{16,17} The applied field alters the distribution function of the holes and hence modulates the absorption. An equivalent effect can be produced by raising the lattice temperature, and this is used to calibrate the field effect.

The details of the scheme for probing the distribution function of the hot carriers can now be discussed. An idealized situation is considered. For the warped energy surfaces, we take equivalent spherical energy surfaces in all bands. It is assumed that the energy bands are all

¹⁶ A. H. Kahn, Phys. Rev. **97**, 1647 (1955).

¹⁷ E. O. Kane, Phys. Chem. Solids **1**, 82 (1956).

¹⁸ For transitions between bands 1 or 2 and band 3, only absorption need be considered; the hole population in band 3 can be neglected because the band is at such high energy, and because of the short lifetime of holes transiently excited to that band.

sharply defined,¹⁹ and that *all* the optical transitions are indeed "direct," as the model proposes. With these approximations, a unique relation exists between the energy of the absorbed photon $h\nu$ and the energy of the hole that is excited; e.g., for the 1-3 transition, as illustrated in Fig. 1,

$$h\nu_{1-3}(\mathbf{k}_j) = \epsilon_3(\mathbf{k}_j) - \epsilon_1(\mathbf{k}_j), \quad (1)$$

where the hole is excited from energy $\epsilon_1(\mathbf{k}_j)$ in band 1 to an energy $\epsilon_3(\mathbf{k}_j)$ in band 3 at the same \mathbf{k} value, since the change in \mathbf{k} due to the absorbed photon is negligible. An analogous relation applies to 2-3 transitions. The theory indicates that for equilibrium conditions ($\mathbf{E}=0$), the absorption coefficient $\alpha_T(\lambda)$ at a given photon frequency or wavelength λ , is directly proportional to the hole concentration, $p_T(\epsilon)$ on the related energy surface²⁰ ϵ in band 1 or 2. Thus

$$\alpha_T(\lambda) = c(\lambda)p_T(\epsilon), \quad (2)$$

where $c(\lambda)$ is a wavelength-dependent proportionality coefficient, assumed to be independent of the lattice temperature, indicated by the subscript T . The hot carrier analysis is based on the expectation¹⁻⁵ that an analogous relation holds for hot carriers, with the proportionality coefficient the same as in the equilibrium case,²¹ i.e.,

$$\alpha_E(\lambda) = c(\lambda)p_E(\epsilon). \quad (3)$$

The hot-carrier distribution, $p_E(\epsilon)$, can then be obtained from measurements of the hot-carrier absorption spectrum at any \mathbf{E} , once the proportionality coefficient $c(\lambda)$ is determined. The latter may be obtained from measurements of the equilibrium absorption coefficient and calculation of the corresponding equilibrium carrier

distribution which is Maxwellian:

$$p_T(\epsilon_i) = [2P_i\epsilon_i^{1/2}/\pi(kT)^{3/2}] \exp(-\epsilon_i/kT), \quad (4)$$

where the total hole concentration in the i th band ($i=1$ or 2) is

$$P_i = P[m_i^{*3/2}/(m_1^{*3/2} + m_2^{*3/2})].$$

P is the total hole concentration in both bands, and m_1^* and m_2^* are the effective masses (assumed constant) in the respective bands.

To associate the correct $p(\epsilon)$ with the corresponding $\alpha(\lambda)$ the relation between λ and ϵ from Eq. (1) must be known, i.e., the band structure in Fig. 1 must be determined. To accomplish this an empirical approach was adopted,²² requiring auxiliary measurements of the dependence of the equilibrium absorption spectrum on T . Applying Eqs. (2) and (4) to such data, we note that plots of $\ln[\alpha_T(\lambda)T^{3/2}]$ versus $1/T$ for each wavelength should give straight lines whose slopes yield the energy ϵ corresponding to any λ . The empirical determination of the relation between λ and ϵ enabled us to apply Eq. (1) to determine the shape $\epsilon_3(k)$ of band 3 in Fig. 1, in terms of the better known parabolic shape of band 1.

The various assumptions comprising the idealized situation were explicitly described above. The degree to which these are in fact violated is known in some instances, not in others. We shall postpone a full evaluation of the difficulties until we have applied the present analysis to the experimental results in Secs. VI and VII.

III. MODULATION OF INFRARED TRANSMISSION BY HIGH-FIELD PULSES

3.1. Description and Conditions of the Experiment

The primary experimental objective is the measurement of the infrared absorption coefficient of hot carriers in p -type germanium. The hot carriers are produced by pulses of high electric field strength, and consequently it is the pulse change in the absorption coefficient which must be measured. The schematic experimental arrangement is shown in Fig. 2. The germanium sample sits in a gas exchange cell of a liquid-nitrogen Dewar. Radiation from the monochromator is focused on the sample, partially transmitted, and is then refocused on a cooled (77°K), InSb barrier detector. When a short pulse of

¹⁹ Broadening of the split-off band 3 due to short lifetime of holes excited to this band, is neglected. For discussion of such broadening effects see T. P. McLean and E. G. S. Paige, *Proceedings of the International Conference on Physics of Semiconductors, Exeter, 1962* (The Institute of Physics and the Physical Society, London, 1962), p. 450, and also Ref. 3.

²⁰ For warped energy surfaces, the situation is more complicated; the correlation of $\alpha(\lambda)$ is not to hole concentration on a constant energy surface in band 1 or 2, but to hole concentration on the surface of constant energy difference, between bands 1 or 2 and 3.

²¹ There are two conditions for the validity of Eq. (3). (a) It is necessary that the band structure and the transition probabilities be independent of \mathbf{E} , i.e., that the latter influence only the distribution function of the carriers. This expectation is reasonable since the maximum field strength employed here was 2800 V/cm, and most of the analyses were made for $E < 2000$ V/cm. The final results, in the range $150 < E < 2800$ V/cm, produced no surprises of such a nature as to cause us to question this basic assumption. (b) The distribution of the hot carriers on the various surfaces of constant energy must be nearly isotropic if the absorption coefficient is to be independent of the state of polarization of the light. However, as a consequence of the work to be reported here, based on the use of Eq. (3), we realized that in fact the hot-carrier distributions were quite anisotropic, and hence that Eq. (3) was not strictly correct. The additional analysis required to obtain the correct relation between $\alpha_E(\lambda)$ and $p_E(\epsilon)$ is given in Ref. 4. Such analysis shows that the error in using Eq. (3) is relatively small, and within the experimental errors in the measurements. (Ref. 4.) Consequently we shall not give this approximation further consideration in this paper.

²² In principle, the desired relationships can be obtained by applying Eq. (1) to the valence band structure theoretically derived by Kane. (Ref. 17.) However, while the theory adequately explains the basic details of the absorption spectrum, there remain appreciable quantitative discrepancies. Kane attributes a major portion of these to uncertainties in the structure of the split-off band 3, due to the approximations in the theoretical analysis. Also, Kane's description of the valence bands includes the warping of the energy surfaces. For warped surfaces, unique hole energies cannot be associated with each photon wavelength. Of course this difficulty will appear also in the empirical approach, but there we hope to obtain an appropriately weighted value for ϵ for each λ . We note that M. A. C. S. Brown *et al.* (Refs. 2 and 3) use an empirical calibrating procedure which is different from ours, and yields much less detailed information.

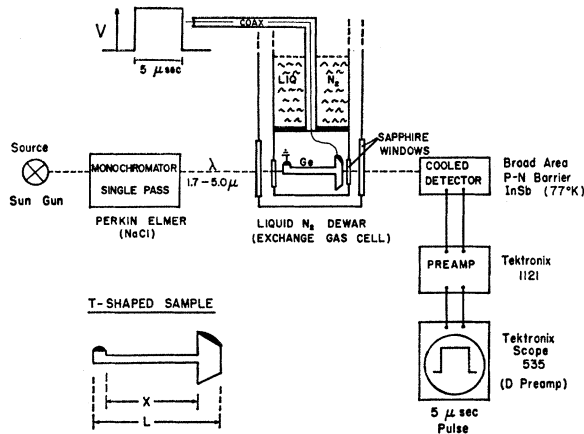


FIG. 2. Schematic experimental arrangement for studying modulation of infrared transmission by pulsed hot carriers in *p*-type germanium.

high voltage is applied to the Ge sample, there is a change in the transmitted intensity ΔI_T , which produces a pulse response in the detector. This pulse is amplified, displayed on the oscilloscope and photographed. With the high voltage switched off, a 13-cps mechanical chopper in front of the light source is activated, and the transmitted light intensity, I_T at zero field, is measured in the same system. The change in the absorption coefficient, $\Delta\alpha_E(\lambda)$ is calculated from $\Delta I_T/I_T$. We shall consider below some special details and conditions of the modulation experiment, especially since modulation of infrared radiation by hot carriers may be useful for its own sake.

a. Pulse Length

The high-voltage pulses applied to the sample must be long enough to heat the carriers to a steady-state distribution and permit the modulated light to pass completely through the sample, but not so long as to heat the sample appreciably. The lower limit is $<10^{-10}$ sec, dictated by the energy relaxation time of the hot carriers, or the transit time of light, whichever is longer. The practical limitation in the present case is set by the response time of the InSb detector, which is about 1 μ sec. The upper limit is set by the carrier concentration in the sample. With pulses of 5- μ sec length, repeated at intervals of about 3 sec, applied to samples with carrier concentration in the range of $\sim 10^{15}/\text{cm}^3$, excessive sample heating could be avoided. The pulses were obtained by discharging a pulse forming network through a hydrogen thyratron across a matching impedance of 10 Ω .

b. Temperature and Carrier Concentration

The choice of ambient temperature and carrier concentration are interrelated, and represents a compromise between partially conflicting requirements. It is desirable for the lattice temperature to be sufficiently low

and the mobility of the carriers high, so that appreciable carrier heating can be obtained even at $E \ll 10^8$ V/cm. However, if the temperature is too low, there is extensive freezeout of carriers. Then the high field will not only heat the free carriers, but also liberate bound ones, thereby complicating the analysis of the absorption changes and of the distribution function. Most of the experiments were made at 77°K, which served as a convenient compromise. At this temperature, the experiments were limited to samples with hole concentrations P in the range 5×10^{14} to $5 \times 10^{15}/\text{cm}^3$. If P is much smaller, the free carrier absorption becomes too small to measure accurately. If P is larger, then (1) an appreciable fraction will freeze out, (2) lattice heating becomes stronger, thus requiring shorter pulse lengths than may be compatible with the rest of the system, and (3) the sample resistance becomes so low that it is difficult to apply suitably high voltages.

c. Sample Shape and Dimensions

The choice of sample dimensions is tied to that of carrier concentration. The path length for the radiation must be sufficiently long to ensure measurable absorption for the given hole concentration. The cross section is determined by the requirement that the sample resistance be sufficiently high ($>$ few ohms) if high voltages are to be obtainable with the given pulse circuitry. Most of the experiments reported here were made with samples having the T shape shown in Fig. 2. Subsequently a simple rectangularly shaped sample was found to be equally satisfactory. The light passed through the long axis of the T, parallel to the electric field direction, and unobscured by the electrical contacts, as shown in the figure. The sample dimensions along the light path were approximately $15 \times 1 \times 5$ mm³, with the long axis chosen parallel to one of the principal crystallographic directions. The samples were lapped to size and etched in CP4, and the far end surfaces were optically polished. The contact areas were lapped with 600-grit carborundum, gold plated, and finally covered with In solder. This procedure usually gave the desired Ohmic, noninjecting contacts. The samples were electrically probed to define the region of high field and of effective modulation of the transmitted radiation.

d. Optics

It was necessary to use an intense light source to obtain sufficient pulse signal with the available detector system. The requirement was satisfied by a "sungun"²³ at $\lambda < 4 \mu$; a globar source was superior at longer wavelengths. A single pass monochromator (Perkin-Elmer, Model 98) was used. Most of the measurements were made with a NaCl prism. The requirements of high intensity on the narrow width of the sample for the hot-

²³ The "Sungun" is manufactured by General Electric and by Sylvania. It has a tungsten spiral filament in a quartz envelope and can be operated at 600 W.

carrier measurements limited the resolution to about 0.15μ . For better resolution in the 3.6 – 5.5μ range, a LiF prism was used.

e. Detection and Measurement of Output Pulse

The requirements on the detector are sensitivity in the 2 to 6μ range, and fast response, of the order of $1 \mu\text{sec}$. These requirements were most adequately met by a cooled (77°K) broad area, diffused junction InSb detector.²⁴ The latter was biased near zero voltage with the unmodulated light incident on the detector. The modulated signals from the detector were fed through a Tektronix 1121 preamplifier usually to the D amplifier of a Tektronix 535 oscilloscope. Bouncing of the pulse signal due to low-frequency noise necessitated photographing of single pulses. The output pulse from the detector, somewhat slowed down by a $1\text{-}\mu\text{sec}$ response time, nearly duplicates the voltage pulse applied to the germanium sample. Distortion of the pulse shape, which complicated the problem of measuring the pulse amplitude, could be attributed to heating of the sample by the voltage pulse.²⁵ The heating of the sample affects the amplitude of the detector output pulse during the time the field is applied to the sample, and adds a long tail to the output pulse corresponding to the modulation of the transmission of infrared through the sample during the thermal relaxation after the field pulse is terminated. The tail in the output pulse is not of concern; in fact, it is even helpful for estimating the ultimate changes in lattice temperature. To minimize the effect of sample heating on the determination of the amplitude of the main detector pulse, the amplitude was read early in the pulse, at about 2 - or $3\text{-}\mu\text{sec}$ mark; it was measured from the original zero level. We observed that the modulation effect due to lattice heating was much less apparent on the main pulse (while the carriers were hot), then on the tail after the field is shut off. A related effect occurs in the study of hot carrier mobility. The mobility of hot carriers is much less sensitive to change in lattice

temperature, than is the mobility at zero field.²⁶ This effect can be explained very simply. The hot carriers at the high fields interact primarily with phonons of relatively high energy, which are not appreciably excited thermally; since the dominant hot carrier interaction with the lattice is via spontaneous phonon emission (instead of phonon absorption and induced phonon emission) the dependence of the hot carrier properties on lattice temperature is suppressed.

3.2. Magnitude and Spectral Dependence of Intensity Modulation

The magnitude of the modulation in transmitted intensity due to hot carriers, $\Delta I_T/I_T$, is illustrated in Fig. 3 for extremes of low and high field strengths of 130 and 2800 V/cm . For these results, \mathbf{E} is along the $[111]$ direction, $T=77^\circ\text{K}$, and $P=1.9 \times 10^{18} \text{ holes/cm}^3$. For the highest fields, and for wavelengths near 3.0 and 4.0μ , the modulation is nearly 50% . Changes down to a few percent are measurable. The negative modulation, corresponding to increase in absorption, is attributed to an increase in density of holes at high energies. The positive modulation is attributed to decrease in hole density at low energies in the band. As indicated in the figure, the 1–3 transitions correspond to wavelengths shorter than 4.3μ , and the 2–3 transitions to wavelengths longer than 4.3μ . For both of these transitions, a separate range of positive and negative modulation is

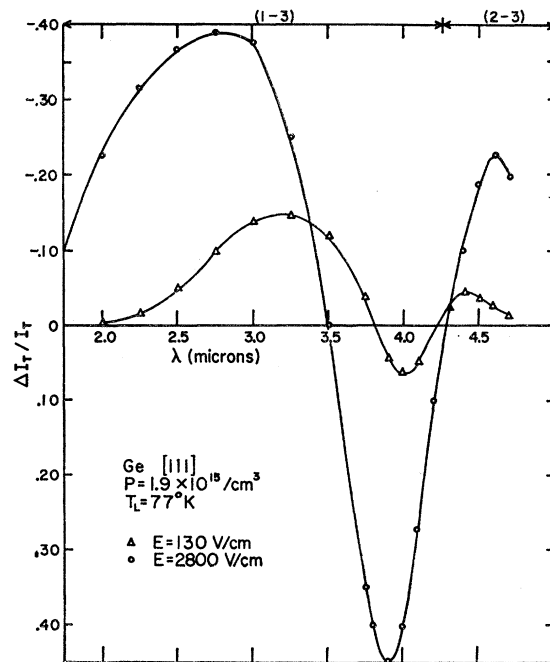


Fig. 3. Spectrum of the fractional modulation of transmitted light intensity at minimum and maximum field strengths used in this experiment. Heavy (1–3)- and light (2–3)- hole transition ranges are shown.

²⁶ D. M. Brown and R. Bray (unpublished).

²⁴ The detector, model 3000, Texas Instruments, Inc., has a $D^*(500,900,1) \approx 10^{10} \text{ cm-cps}^{1/2}/\text{W}$.

²⁵ An occasional source of distortion was radiation *sometimes* observed to be emitted from the Ge samples at high-field strength. Superposition of this radiation, if present, on the transmitted pulse distorts the latter, especially since the emission signal goes directly to the detector. One type of radiation, that due to recombination of injected carriers was easily detectable, and could usually be avoided by simply refinishing the end contacts to suppress injection. A more serious matter was emission radiation occurring in a broad band at longer wavelength. The intensity of such emission rose nearly linearly in time, reaching a peak about $1 \mu\text{sec}$ after the voltage pulse begins to drop; its subsequent decay was initially rapid, but was followed by a slower transient with about $10 \mu\text{sec}$ decay time. The emission intensity was much stronger at 77°K than at room temperature, it increased approximately linearly with field strength. The presence of the emission was strongly dependent on the details of sample preparation, and appeared to be due to surface effects. Care was taken to ensure that for the desired measurements, the emission signal was very much less than the modulated transmission signal, or not observable at all. Broad-band emission has also been reported by M. A. C. S. Brown, Phys. Chem. Solids **23**, 135 (1962).

to be expected. While such behavior is observed for 1-3 transitions, the region of positive modulation is missing for the 2-3 transitions. The latter effect may be attributed to inadequate resolution, both instrumental and inherent.¹⁹

The modulation in transmitted intensity was studied in detail as a function of electric field strength, (a) for two orientations: \mathbf{E} along the [111] and [100] directions, (b) for two carrier concentrations: $1.9 \times 10^{15}/\text{cm}^3$, and $5.9 \times 10^{14}/\text{cm}^3$, and (c) as a function of the direction of polarization of the light with respect to the electric field direction. The results will be described in terms of the changes in absorption cross section obtained from the $\Delta I_T/I_T$ data.

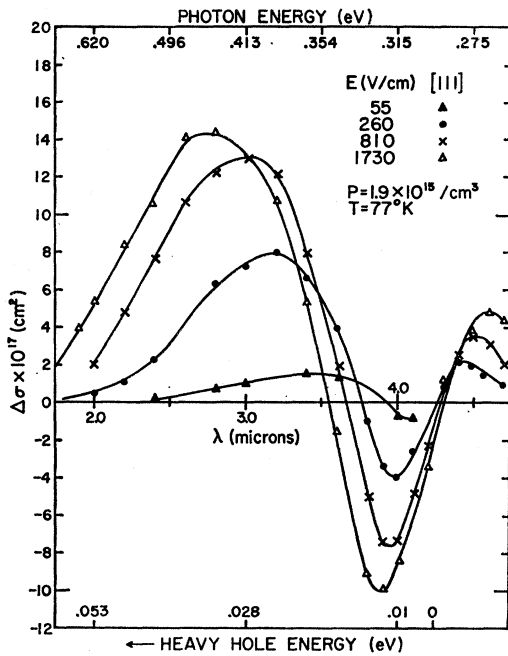


FIG. 4. Spectrum of change in absorption cross section for various electric field strengths. The energies of the heavy holes participating in the absorption are shown. \mathbf{E} is in the [111] direction.

3.3. Change in Absorption Coefficient

The intensity transmitted at zero field, I_T is related to the absorption coefficient of the material by the usual relation

$$I_T = I_{\text{inc}} \frac{(1-R)^2 \exp(-\alpha_0 L)}{1 - R^2 \exp(-2\alpha_0 L)}, \quad (5)$$

where I_{inc} is the intensity incident on the sample, α_0 is the absorption coefficient at zero field, L is the over-all absorption length of the sample, and R is the reflectivity of Ge, ~ 0.35 . When the electric field is applied, the change in transmitted intensity, (ΔI_T) is related to the change in absorption coefficient $\Delta\alpha_E$ by the equation

$$\frac{(\Delta I_T)_E - I_T}{I_T} = \Delta I_T / I_T = B e^{-x\Delta\alpha_E} - 1, \quad (6)$$

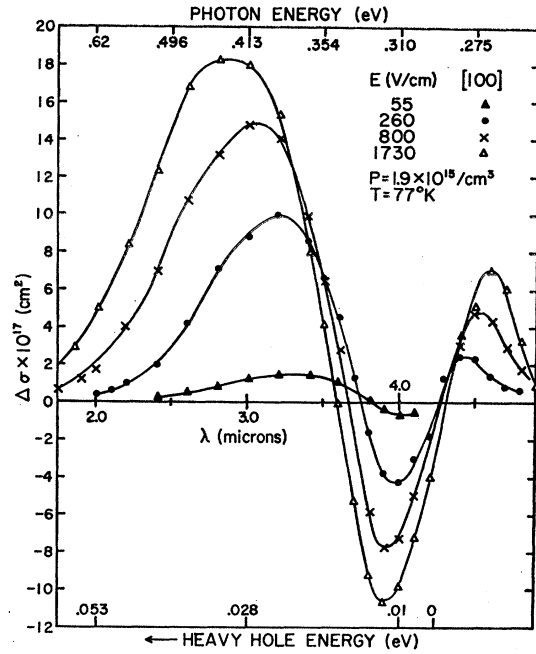


FIG. 5. Same as Fig. 4, but with \mathbf{E} in [100] direction.

where x is the effective absorption length over which the field strength is equal to \mathbf{E} (see Fig. 2); B , a factor nearly equal to 1, is given by

$$B = (1-A)/(1 - A e^{-2x\Delta\alpha_E}) \quad (7)$$

and

$$A = R^2 e^{-2L\alpha_0}.$$

Equations (6) and (7) may be solved directly for $\Delta\alpha_E$. We define the change in the absorption cross section $\Delta\sigma_E$ as the ratio of $\Delta\alpha_E$ to the total carrier concentration.

a. Dependence on Magnitude and Orientation of Electric Field Strength

The $\Delta\sigma_E$ spectra for a few selected field strengths, $\mathbf{E} = 55, 260, 800,$ and 1730 V/cm, are shown in Fig. 4 for $\mathbf{E} \parallel [111]$ and in Fig. 5 for $\mathbf{E} \parallel [100]$. In both cases the radiation is propagated parallel to \mathbf{E} . The study was made with Ga-doped Ge, containing 1.9×10^{15} holes/cm³, for the two oriented T-shaped samples.

We note in the 1-3 transition range, the shift of the absorption to shorter wavelength with increasing field. This simply represents the shift in heavy holes to higher energies in band 1. In the present form, this data is ready for direct translation into distribution functions in Sec. VII. The heavy hole energies shown on the lower horizontal axes of the figures, are obtained from the analysis to be given in Sec. VI.

Comparison of the data in Figs. 4 and 5, for the two orientations, show that they are not identical at corresponding field strengths, for $\mathbf{E} > 260$ V/cm. For example, the peak values of $\Delta\sigma_E$ (near $\lambda = 3 \mu$) are noticeably larger in the [100] direction. An orientational an-

isotropy has also been observed in the field dependence of the mobility, the high field mobility being generally higher for the [100] direction than for the [111] direction,²⁷ and the divergence becoming noticeable at about the same field strength as for the absorption effect. The existence of the orientation dependence in both cases is presumed to be related to the warping of the energy surfaces in the valence bands, but its presence may also reflect the nature of the hot-carrier effect (Sec. VIII).

b. Dependence on Carrier Concentration

The absorption cross section was measured only at two hole concentrations, 1.9×10^{15} and $5.9 \times 10^{14}/\text{cm}^3$. A comparison was made at equivalent power input per hole $\mu \mathbf{E}^2$, rather than at equal \mathbf{E} . No significant variation in magnitude or shape of the $\Delta\sigma_E$ spectrum was found in the range $260 < \mathbf{E} < 1300$ V/cm. By contrast, Brown *et al.*³ report a strong variation in absorption cross section in the concentration range 0.6×10^{15} to 9×10^{15} holes/cm³, at $\mathbf{E} < 350$ V/cm, and $T = 93^\circ\text{K}$. For increasing carrier concentration, they report smaller values of $\Delta\sigma_E$, hence, smaller carrier heating effect, at equivalent power input per carrier. We are not aware of any explanation for this difference in results in the two investigations.

c. Dependence on Polarization of Light

For completeness, we report that the absorption is anisotropic for hot carriers, being dependent on the direction of polarization of the light with respect to the field direction for a given crystallographic direction. The effect was investigated only for the 1-3 transitions. It was found that the absorption is greatest when the polarization vector of the light is perpendicular to the field direction. This is consistent with our observation that for unpolarized light, the hot-carrier absorption coefficient is greatest when the propagation direction is parallel to \mathbf{E} . We have given brief analyses of this result elsewhere which shows that it is related to the anisotropy in the distribution of hot carriers on surfaces of constant energy.^{4,5}

IV. TEMPERATURE DEPENDENCE OF EQUILIBRIUM ABSORPTION COEFFICIENT

The motivation for the study presented in this section was given in Sec. II, where it was shown why an empirical analysis of the valence band structure was a necessary prerequisite for determining the hot carrier distribution functions, and how such an analysis could be made from the dependence of the equilibrium absorption coefficient on the temperature. The data also served for a preliminary attempt to obtain hot carrier temperatures, as described in Sec. V.

Previous measurements of the intervalence band ab-

sorption coefficient were inadequate for our purpose. The very extensive data of Kaiser *et al.*²⁸ were obtained on material with relatively large impurity concentration, $P \sim 10^{17}/\text{cm}^3$. At such concentrations the absorption is concentration-dependent, and hence the transitions are no longer purely "direct" according to the work of Newman and Tyler.²⁹ Measurements on purer samples by Newman¹⁷ and by Briggs and Fletcher³⁰ yield absorption cross sections differing from each other by about 50%. In the present experiments, the absorption coefficient was determined on two samples with hole concentrations of $2.3 \times 10^{15}/\text{cm}^3$ and $5.7 \times 10^{15}/\text{cm}^3$, pure enough to expect that the absorption cross sections are independent of impurity concentration. The data were taken as a nearly continuous function of temperature, in the range $77^\circ \leq T \leq 300^\circ\text{K}$, at some 19 wavelengths in the range $1.7 \leq \lambda \leq 5.0 \mu$, corresponding to the 1-3 and 2-3 transitions.

4.1. Experimental Method

The method of measuring the free hole absorption coefficient was dictated by the fact that the absorption is very weak over much of the wavelength range, particularly at the lower temperatures, and therefore strongly dependent on the exact specification of the reflectivity and the surface conditions. In this case, the usual method of measurement, sample in-sample out of beam, is particularly susceptible to error. Instead, a comparative method was employed; the transmitted intensity was measured in turn through a relatively pure piece of *n*-type Ge ($35 \Omega\text{-cm}$ at 300°K) and through two pieces of *p*-type material. All three pieces were cut to have identical rectangular dimensions, ($3 \times 4.5 \times 9.4$ mm³) joined together with an adhesive to form a unit, and the ends of the unit were lapped and optically polished. The unit was mounted in the same Dewar used for hot carrier measurements, and the ratios of transmitted intensity $S = I_p/I_n$ through the *p*- and pure *n*-type samples were determined. The absorption coefficient for the *p*-type samples were obtained from the following relation:

$$S = \frac{I_p}{I_n} = e^{-\alpha_p L} \left[\frac{1 - R^2 e^{-2\alpha_n L}}{1 - R^2 e^{-2(\alpha_p + \alpha_n) L}} \right]. \quad (8)$$

The term in brackets takes account of multiple reflections in the samples. R is the reflectivity, L is the absorption length of the sample, α_p is the intervalence band absorption coefficient for free holes, and α_n the absorption coefficient due to all absorption processes in the pure *n*-type Ge. Except near the intrinsic absorption band edge, α_n was determined to be less than 0.01 cm^{-1} (by the usual sample in-sample out of beam method),

²⁸ W. Kaiser, R. J. Collins, and H. Y. Fan, Phys. Rev. **91**, 1380 (1953).

²⁹ R. Newman and W. W. Tyler, Phys. Rev. **105**, 885 (1957).

³⁰ H. B. Briggs and R. G. Fletcher, Phys. Rev. **91**, 1342 (1953).

²⁷ D. Deutsch, D. M. Brown, and R. Bray (unpublished); see W. E. K. Gibbs, J. Appl. Phys. **33**, 3369 (1962).

and was dropped from the above equation. The coefficient α_p was then obtained from a graph of S versus α_p . Correction for α_n in the band edge, permitted extension of intervalence band absorption measurements to short wavelengths (1.7μ) within the fundamental absorption range.

The technique has several valuable features: (1) S and hence α_p are obviously rather insensitive to the choice of R and its possible dependence on wavelength and temperature. R is assumed to be the same for all samples in the unit, which were prepared simultaneously and identically. (2) In standard transmission measurements, the beam falling on the detector must be refocused if a long sample is moved in and out of the beam. In the present arrangement, all the samples have the same length, and no refocusing is necessary irrespective of the optical path in the samples.

A complete temperature run between 77 and 300°K was made at each selected wavelength, the transmission at a given wavelength being measured in turn through the three samples. The samples were warmed up very slowly, and the transmission data and the temperature were recorded continuously. A single-pass Perkin-Elmer monochromator, Model 98 was used, with NaCl and LiF prisms. Narrow slits ≈ 0.05 mm gave better resolution here than in the hot carrier measurements, where greater intensities were necessary. The detector was a Reeder thermocouple, operated with the standard 13-cps Perkin-Elmer amplification circuitry into a dc recorder.

4.2. Results

Absorption spectra at selected temperatures are shown in Fig. 6 for the sample with $P = 5.7 \times 10^{15} \text{ cm}^{-3}$. Comparison of the curves for this sample with those for the purer sample ($P = 2.3 \times 10^{15} \text{ cm}^{-3}$) showed that $\alpha_T(\lambda)$ for the former was 2.55 ± 0.06 larger than for the latter. This is in good agreement with the ratio of carrier concentrations from Hall effect measurements at 7000 G at 77°K, which was 2.48. A comparison of our absorption cross sections with those of previous workers^{17,30} shows that in general our results are intermediate between the others, except near 77°K where they nearly coincide with those of Newman.¹⁷ The general shapes of the absorption spectra of the various workers are in good agreement, suggesting that discrepancies may be due mainly to incorrect specification of the carrier concentration. In analyzing our Hall measurements, we benefited from the extensive analyses made by Brown and Bray.¹⁴ The discrepancies between theory and experiment, discussed by Kane¹⁷ on the basis of Newman's data are not significantly altered by the present results.

The changes in shape of the absorption curves with temperature are due mainly to two factors: (1) the variation with temperature of the distribution function of the holes in bands 1 and 2, and (2) the complicated dependence of the transition probability on the wave vector \mathbf{k} . Decreases in α_T with increasing T reflect de-

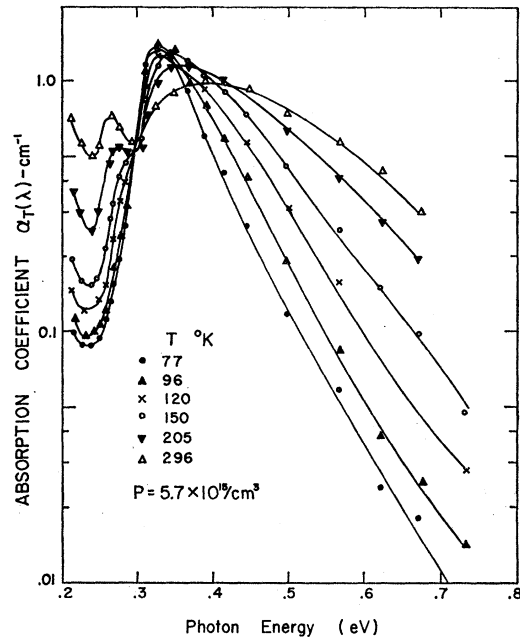


Fig. 6. Equilibrium absorption coefficient spectra for different lattice temperatures.

creases in the hole concentration at low band energies. The holes lost at lower energies are transferred to higher energies in the band where they cause the absorption to increase strongly with increasing temperature. For detailed discussion we refer to the work of Kane.¹⁷ The absence of a decrease in α with increasing T in the 3-2 transitions at photon energies < 0.29 eV has been discussed by McLean and Paige.^{19,3}

V. PRELIMINARY ANALYSIS: SEARCH FOR A HOT CARRIER TEMPERATURE

The objective of the analysis presented here is to determine whether the hot-carrier distribution function is Maxwellian; if it is, then a carrier temperature T_c can be specified and associated with each value of the applied field strength. The procedure followed consisted of seeking a correspondence between an absorption spectrum $\alpha_E(\lambda)$ at a given field strength \mathbf{E} , at sample temperature $T = 77^\circ\text{K}$, and the absorption curve $\alpha_T(\lambda)$ at some lattice temperature $T > 77^\circ\text{K}$, at $\mathbf{E} = 0$. Should a 1:1 correspondence exist, the implication would be that the hot-carrier distribution is Maxwellian, with a temperature equal to that for the matching equilibrium curve. The underlying assumption is that the effect on the absorption spectrum of either applying field or raising the lattice temperature is due solely to the change in the carrier distribution function. We note that for this analysis it is not necessary to know details of the band structure, such as the degree of warping, or what carrier energy is associated with a given photon wavelength. It suffices to know only that the absorption is due to direct intervalence band transitions.

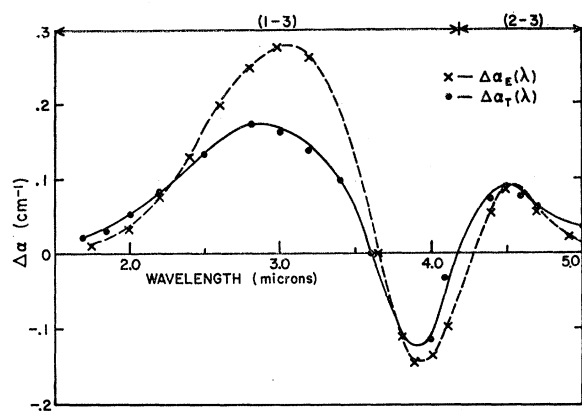


FIG. 7. Comparison of change in absorption coefficient $\Delta\alpha_E(\lambda)$ for $E=800$ V/cm at $T=77^\circ\text{K}$ with change in equilibrium absorption coefficient $\Delta\alpha_T(\lambda)$ due to increase in lattice temperature from 77 to 170°K . The failure to find a 1:1 correspondence of the two spectra is indicative of the non-Maxwellian character of the hot-carrier distribution.

In Fig. 7 we compare a curve of $\Delta\alpha_E(\lambda)$ at $E=800$ V/cm, with one of $\Delta\alpha_T(\lambda)$, where the latter corresponds to a change of lattice temperature from 77 to 170°K . It is evident that there is a fair qualitative agreement in the wavelength dependence of the two curves, but that they do *not* match quantitatively. Attempts to obtain a

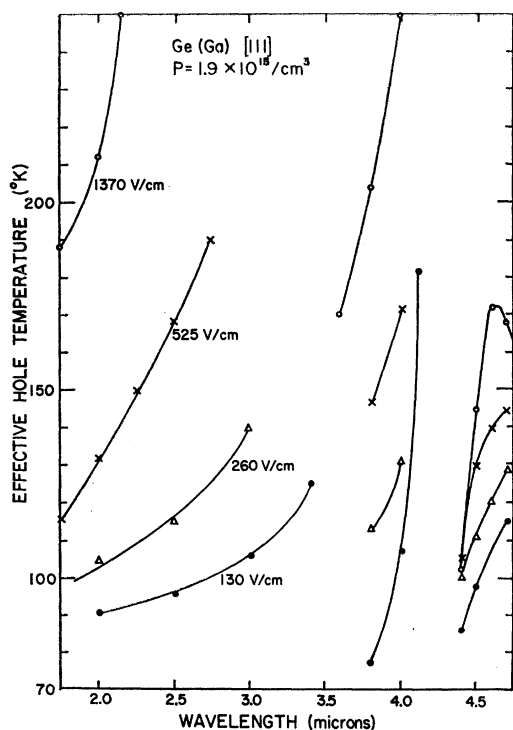


FIG. 8. Variation of the effective temperature of hot holes with probing photon wavelength, at the various indicated field strengths. Effective temperature is defined by matching $\alpha_E(\lambda)$ with $\alpha_T(\lambda)$, as described in text. The variation of effective temperature with wavelength at a given E is a measure of deviation from Maxwellian distribution.

better fit, by choosing $\Delta\alpha_T(\lambda)$ curves for different increments in lattice temperature, yield no improvement but merely alter the regions of overlap. From the failure to find the desired 1:1 correspondence between field and temperature measurements, we deduce that the hot-carrier distribution is not Maxwellian.

It is instructive to investigate the *degree of divergence* from a Maxwellian distribution for the hot carriers. We may ascribe an effective carrier temperature T_e to each point on the $\alpha_E(\lambda)$ curve; T_e is defined by finding for a given $\alpha_E(\lambda)$ an equal $\alpha_T(\lambda)$ at the same wavelength. For this purpose we use the data obtained on the variation of the equilibrium absorption coefficient with lattice temperature between 77 and 300°K . The variation of T_e with wavelength may be obtained for each field strength. A family of such curves is shown in Fig. 8. There are gaps in the curves where T_e was not definable at those wavelengths where no value of $\alpha_T(\lambda)$ existed (at any lattice temperature) which was equal to the given value of $\alpha_E(\lambda)$.³¹ This means that at certain points in the energy band the hole population produced by the field is incompatible with a Maxwellian distribution at any temperature—for the given total hole concentration.

Only if the values of T_e obtained at any E were independent of λ would it be meaningful to ascribe a temperature to the hot carriers. Nevertheless, the observed variation of the parameter T_e with λ is of some value.³² From the T_e curves we may draw the following interesting, but very qualitative conclusions: (1) The average carrier "temperature" is not drastically increased at high-field strengths. (2) Particularly low effective "temperatures" are deduced in the short wavelength range of the data near $2\ \mu$, from the small increase in absorption there, even at high-field strengths. This region of the spectrum corresponds to the heavy holes in the higher energy range of band 1. (The energy will be specified with the aid of the analysis in Sec. VI.) The implication is that relatively little increase in population is produced at high hole energies by the action of the field, as compared to the effect of raising the lattice temperature even by moderate amounts. (3) The range of T_e for the heavy holes ($1.8 < \lambda < 4.3\ \mu$) and for the light holes ($4.3 < \lambda < 4.8\ \mu$) is not very different at the two lowest field strengths. At progressively higher field strengths, the effective temperatures of the heavy holes appear to increase much more rapidly than for the light holes. This can also be interpreted to mean that the relative population of the light holes at higher fields is decreasing. Unfortunately, this is the only point where comparison of light and heavy hole properties was possible; details of the energy distribution function could be determined only for the heavy holes.

³¹ At some wavelengths, $\alpha_E(\lambda)$ could not be matched with $\alpha_T(\lambda)$ because the latter was not measured at $T > 300^\circ\text{K}$.

³² Somewhat different values of T_e would have been obtained had we used a different direction of propagation of the light with respect to the field direction because of the anisotropic distribution of hot carriers on energy surfaces. However, the qualitative conclusions given here would still be valid.

We conclude, from the relatively weak increase in carrier "temperature" with field, and from the partial suppression of the high-energy tail of the distribution, that the hot carriers are subjected to strong inelastic scattering, which may be attributed to strong optical phonon interactions. These conclusions will be substantiated and extended by the more quantitative determination of the distribution functions and the subsequent analyses in the following sections.

VI. EMPIRICAL ANALYSIS OF VALENCE BAND STRUCTURE

As a prerequisite for determining the energy distribution functions of the hot carriers, it is necessary to obtain an empirical description of the valence band structure, or more specifically the relation between photon energy and hole energy. According to the scheme outlined in Sec. II, plots of the quantity $\ln[\alpha_T(\lambda)T^{3/2}]$ versus $1/T$ should give straight lines, with the slopes yielding the hole carrier energy corresponding to the given photon

TABLE I. Correspondence between heavy-hole energy and wavelength of absorbed photons for 1-3 transitions.

$\lambda(\mu)$	$h\nu_{1-3}(\text{eV})$	$\epsilon_1(\text{eV})$
1.7	0.73	0.0635
1.85	0.67	0.0578
2.0	0.62	0.0529
2.2	0.56	0.0460
2.5	0.495	0.0383
2.8	0.440	0.0318
3.0	0.412	0.0278
3.2	0.386	0.0236
3.4	0.363	0.0197
3.6	0.342	0.0162
3.8	0.325	0.013

energy. Such plots, for the various indicated photon energies, are presented in Figs. 9 and 10, using the equilibrium absorption data. The ordinates are normalized to the value of $[\ln\alpha_T(\lambda)T^{3/2}]$ at 300°K. The data in Fig. 9 correspond to the 1-3 absorption band, and those in Fig. 10 predominantly to the 2-3 absorption band, with possible overlap with the 1-2 absorption band at the longer wavelengths. The slopes are not constant over the entire temperature range at any wavelength. Consequently, precise values of carrier energies in bands 1 and 2 can not be specified and associated unambiguously with each photon energy. Nevertheless, there is clearly appreciable distinction in slopes for the various curves, and if we are willing to accept limitations on the resolution, quite useful descriptions of the distribution functions can be obtained. It is important however, to spell out what approximations are to be made, and the limitations within which the hot carrier distribution functions can be analyzed.

We note that the slopes are nearly constant for that portion of the data in the temperature range $100^\circ\text{K} < T < 300^\circ\text{K}$, and for photon energies $0.34 < h\nu < 0.67$ eV,

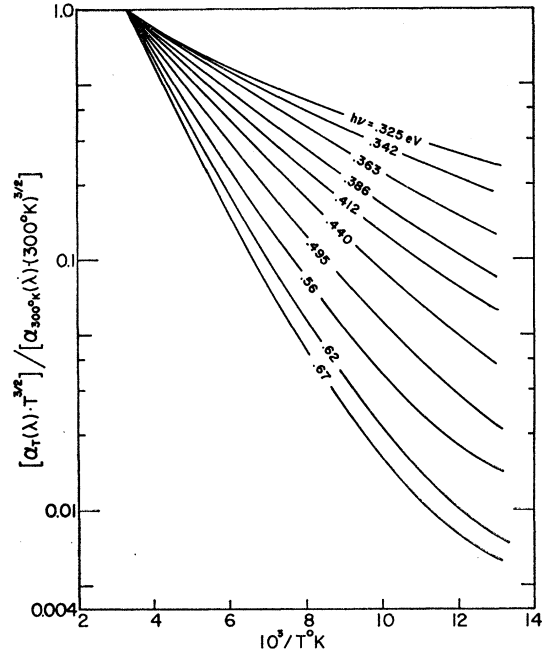


FIG. 9. $\ln[\alpha_T(\lambda)T^{3/2}]$ versus $1/T$ plots for photon energies corresponding to 1-3 transitions. Ordinates are normalized to values at $T=300^\circ\text{K}$. Slopes yield energy of heavy holes associated with given photon energy.

which correspond to the major portion of the 1-3 absorption band in Fig. 9. The values of the energies of the heavy holes, derived from these slopes, are given in Table I, as a function of the corresponding photon energies $h\nu_{1-3}$. The range of heavy hole energy, 0.015 to

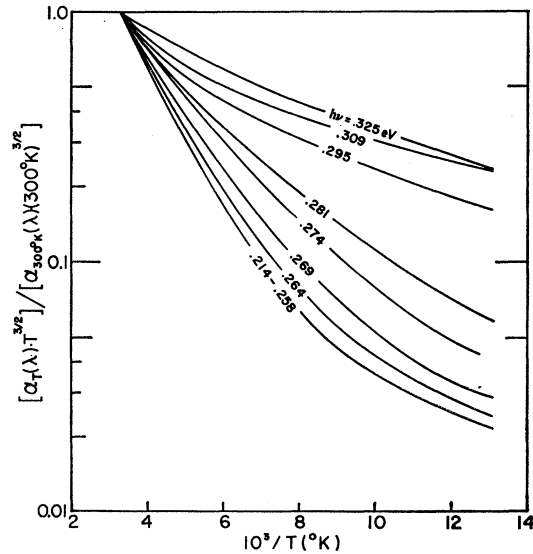


FIG. 10. $\ln[\alpha_T(\lambda)T^{3/2}]$ versus $1/T$ plots for 2-3 transitions and 1-3 transitions of heavy holes with low energies. The ordinates are normalized to values at $T=300^\circ\text{K}$. The nonlinearity of the slopes frustrates the analysis of the distribution functions of light holes.

0.06 eV is covered by this analysis. The nonlinearity of the curves is especially pronounced in Fig. 10 for photon energies $h\nu < 0.34$ eV. This range includes the heavy holes at low energies $\epsilon_1 \lesssim 0.015$ eV, and the whole of the light hole band. For $h\nu \leq 0.258$ eV, no distinguishing slope dependence on photon energy can be obtained. For this range, the present analysis appears to be completely inadequate.

With the data from Table I, a partial picture of the shapes of the energy bands can be drawn. The variation of energy with k^2 for bands 1 and 3 was shown in Fig. 1. Band 1 is drawn as a straight line, corresponding to an average, energy-independent effective mass ratio of 0.35 for the heavy holes. Using this line as a base, the vertical displacement of band 3 on the energy scale is determined by the photon energies $h\nu_{1-3}$ associated with each heavy hole energy in band 1, according to Eq. (1). The energy displacement at $k=0$, is the commonly accepted value of 0.29 eV. Band 3 emerges as strongly nonparabolic in shape.

A similar analysis was attempted for band 2, using roughly estimated values of light hole energy from the slopes of the curves in Fig. 10. The available information was concentrated in a very narrow range of k^2 near $k=0$ and was quite useless for determining the shape of band (2). The shape shown in Fig. 1 was taken from Kane.¹⁷ It was concluded that further analysis of the distribution function of the light holes was not feasible.

As a guide for evaluating the heavy hole results they are compared with those obtainable from Kane's theoretical analysis of the structure of the valence bands. In Fig. 11 are plotted the theoretical curves, derived from Kane,¹⁷ of heavy hole energy ϵ_1 versus $h\nu_{1-3}$ for the three principal crystallographic directions, and for a fourth, " γ " direction which makes equal angles with the other three. The dependence of the theoretical curves on crystallographic direction is a consequence of the warping of the energy surfaces in bands 1 and 3. Therefore a spread of energy values in band 1 is associated with any

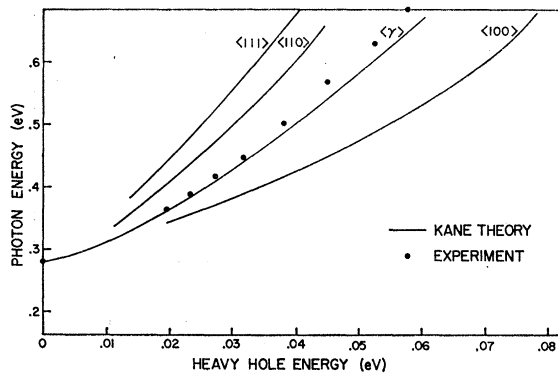


FIG. 11. The points represent the experimentally deduced correlation between heavy hole energy and energy of absorbed photons. The solid curves are obtained from theoretical analyses by Kane (Ref. 17) for the indicated crystallographic directions. For significance of γ direction, see text.

given photon energy. The experimental results from Table I are plotted for comparison. They are in good agreement with Kane's curve for the γ direction. The latter was assigned a greater weight³³ by Kane than all three principal directions combined for the purpose of averaging the absorption over all directions. It follows that the band structure empirically drawn in Fig. 1 is most closely representative of the theoretical γ direction. It seems reasonable to conclude that the experimental results represent *empirically* averaged heavy hole energies to be associated with the respective photon energies.

Finally we consider some reasons for the difficulties in the analysis of the valence band structure:

(1) Probably the dominant factor in the nonlinearity of the $[\ln\alpha_T(\lambda)T^{3/2}]$ curves is the fact that bands 1 and 3 are warped, which prevents a unique hole energy from being associated with a particular photon energy. In this case the weight to be given to contributions to $\alpha_T(\lambda)$ for the different crystallographic directions should shift with temperature, and could account for much of the observed nonlinearity.

(2) The assumption that the structure of the valence bands is temperature-independent may not be completely valid. However, no firm conclusions can be drawn regarding this factor from available work. Kane¹⁷ points out that some increase in curvature of band 3 with increasing T may be expected on theoretical grounds. He finds, however, an inverse effect from an empirical attempt to improve agreement between absorption theory and experiment.

(3) McLean and Paige¹⁹ have pointed out that a broadening of about 0.02 eV should be associated with the split-off band due to the short lifetime of holes excited into this band and very quickly scattered into the upper portions of bands 1 and 2 where the density of states is very high. Such a broadening will have particularly serious effects on the 2-3 transitions which occur in a very narrow range of k , corresponding to a very small energy range in band 3. The broadening should also serve to confuse 1-3 and 2-3 transitions near $k=0$, which is just where the present analysis of carrier energies gave particular difficulty.

(4) According to the absorption model, free carrier absorption is due only to direct optical transitions. However, the contribution to the absorption by indirect transitions can not be completely ruled out, especially where the direct transitions are very weak, at the higher hole energies at low temperature, and near $k=0$, where direct transitions are forbidden.

To conclude, the study of the valence band structure has revealed the limitations in range and resolution within which an analysis of the hot carrier distribution

³³ The weighting was made by considering the surface of a sphere in \mathbf{k} space and assigning a small element of area to whichever of the four computed directions it was closest. The weightings were then made proportional to the area and were normalized.

function is feasible. Only the 1-3 transitions may be regarded as useful for this purpose; even here, the analysis is applicable to heavy holes only in the range 0.015 to 0.06 eV. Nevertheless, as will be evident, quite useful descriptions and applications of the distribution functions can be obtained.

VII. ANALYSIS AND APPLICATIONS OF ENERGY DISTRIBUTION FUNCTIONS OF HOT CARRIERS

7.1. Analysis and Results

To calculate the hot-carrier distribution $p_E(\epsilon)$ from measurements of $\alpha_E(\lambda)$, we attempt to follow the scheme outlined in Sec. II. Using Eqs. (2) and (3) to eliminate the coefficient $c(\lambda)$, we obtain

$$p_E(\epsilon) = [\alpha_E(\lambda)/\alpha_T(\lambda)] p_T(\epsilon). \quad (9)$$

For the relation between λ and ϵ , the data from Table I are used; the ratio $\alpha_T(\lambda)/p_T(\epsilon)$ is calculated from Eqs. (2) and (4). The problem arises that this calibrating ratio is temperature-dependent as demonstrated by the non-linearity of the curves in Fig. 9. We chose³⁴ to evaluate the ratio for such T that $\alpha_E(\lambda)/\alpha_T(\lambda)$ was near unity, which generally meant taking T in the range where $\alpha_T(\lambda)/p_T(\lambda)$ was constant.

As noted in Sec. VI, the determination of $p_E(\epsilon)$ is limited to heavy holes in the energy range $0.015 < \epsilon < 0.06$ eV. At the upper bound the free carrier absorption becomes very weak and the competitive intrinsic absorption becomes dominant. We obtained $p_E(\epsilon)$ at $\epsilon > 0.06$ eV by straight line extrapolation of the function $\ln[p_E(\epsilon)/\epsilon^{1/2}]$ versus ϵ . This gives the extrapolated function an exponential character, $p_E(\epsilon)/\epsilon^{1/2} = D \times \exp(-\epsilon/kT^*)$, where D and T^* are fitted parameters. At the lower bound, $\epsilon < 0.015$ eV, the energy distribution could not be reliably determined, and was therefore

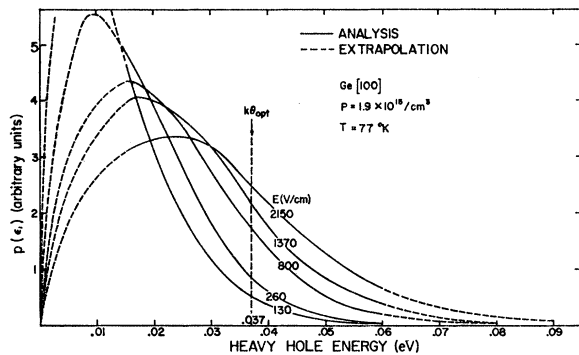


FIG. 12. Experimentally determined energy distributions of heavy holes for the indicated field strengths in [100] direction. The dashed portions represent extrapolated values, as discussed in text.

³⁴ This somewhat arbitrary choice is governed by the assumption that the temperature dependence of the calibrating ratio is mainly due to warping of the bands and not to change in band structure with temperature.

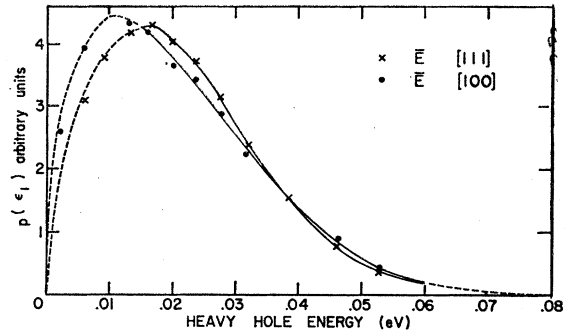


FIG. 13. Comparison of heavy hole distribution for measurements along [100] and [111] direction, at $E=800$ V/cm.

estimated rather arbitrarily. Finally, the total distribution was checked for consistency by determining if the total free hole concentration remained constant at all fields. This quantity was generally about 10% too small at the lower field strengths, and a few percent too large at higher fields. It is expected that the experimental distributions will be most reliable for intermediate field strengths $E \sim 800$ V/cm. At low E , a large proportion of the carriers still have energies below 0.015 eV. At very high E , there is an increasing proportion of the carriers with $\epsilon > 0.06$ eV, and we have to rely too heavily on the extrapolation.

Representative curves of the energy distribution of heavy holes $p_E(\epsilon_1)$ are shown in Fig. 12, for field strengths between 130 and 2150 V/cm. The dashed portions of the curves represent the extrapolations described above. The results shown are for $E \parallel [100]$ at $T=77^\circ\text{K}$, and $P=1.9 \times 10^{18}/\text{cm}^3$. Similarly extensive results were obtained for the [111] orientation. The relatively small differences in the distribution function for the two orientations are illustrated in Fig. 13 for $E=800$ V/cm. We shall now apply the distribution curves to determine various features of the hot carriers.

7.2. Non-Maxwellian Energy Distribution

The non-Maxwellian character of the energy distributions, demonstrated earlier in Sec. V, can now be substantiated. In Fig. 14 the experimentally determined energy distribution at $E=800$ V/cm is compared with a calculated Maxwellian distribution at $T=169^\circ\text{K}$, chosen so as to have the same average energy. The former shows a relative depletion in carrier concentration at both low and high energies, and a piling up of carriers at intermediate energies. From the double crossover of the two curves, it is clear that no Maxwellian distribution, at any other temperature, can match the experimental curve. There are two conditions for the energy distribution to be Maxwellian: (1) sufficient carrier density for carrier-carrier energy exchange rate to be dominant over all other carrier interactions, and (2) small displacement of the distribution function in momentum space by the electric field. For a strongly dis-

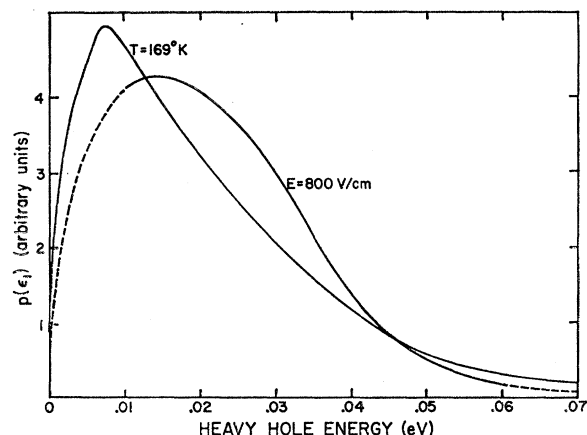


FIG. 14. Comparison of experimental energy distribution of heavy holes at $E=800$ V/cm, and $T=77^\circ\text{K}$ with an equilibrium distribution at $T=169^\circ\text{K}$. The latter is chosen so as to have the same average energy as for the hot-carrier case. E is along [100] direction, and $P=1.9 \times 10^{15}$ holes/cm 3 . The non-Maxwellian character of hot carriers is specifically demonstrated, as is the relative impoverishment of the hot-carrier concentration at high energies.

placed Maxwellian distribution, the energy distribution function can be shown to be non-Maxwellian. Either or both of these conditions are apparently not met in the present case. We shall show in Sec. 7.4 that the distribution is indeed strongly displaced. In Sec. 7.5 the strong energy loss rate of hot carriers to optical phonons will be demonstrated; it is unlikely that carrier-carrier scattering can compete with this process.

7.3 Average Hole Energy

The variation with E of the average energy $\bar{\epsilon}$ of the heavy holes, determined from the various distribution curves, is shown in Fig. 15(a). After an initial rise, $\bar{\epsilon}$ increases rather slowly with E . Even at the highest E shown, $\bar{\epsilon}$ is appreciably smaller than the optical-phonon energy $k\theta_{\text{opt}}=0.037$ eV. The *containment* of the majority

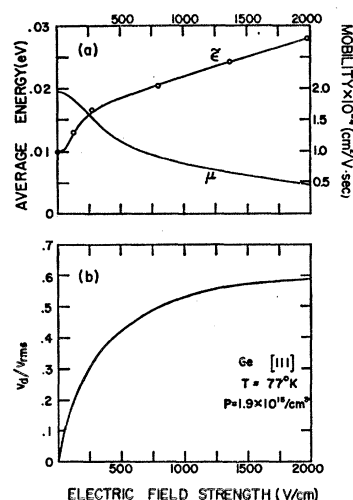


FIG. 15 (a) Field dependence of average energy ($\bar{\epsilon}$) of heavy holes, and of the total hole mobility, μ . (b) Ratio of drift to root-mean-square velocity of holes as a function of field strength. The drift velocity is obtained from μ , and rms velocity from $\bar{\epsilon}$.

of the holes at energies below 0.037 eV, even at $E \sim 2000$ V/cm, is already evident from inspection of the distribution curves in Fig. 12.

The relatively slow increase of average energy with E is indicative of the strength of the inelastic scattering processes. The obvious mechanism for this is the optical phonon interaction. The shapes of the distribution curves are consistent with this conclusion. Strong optical phonon emission by holes at energies above the emission threshold 0.037 eV, would impoverish the high-energy tail of the distribution functions. Quantitative confirmation of the strength of the optical phonon interaction will be provided in Sec. 7.5.

7.4. Displacement of Distribution in Momentum Space

An over-all measure of the displacement of the distribution function in momentum space is given by the quantity, v_d/v_{rms} , the ratio of the drift to the root-mean-square velocity. The drift velocity is obtained from the measured field dependence of the mobility, shown in Fig. 15(a). The rms velocity is calculated from the average energy, which includes the translational energy due to drift. The variation of v_d/v_{rms} with field strength is given in Fig. 15(b). The combination of low average energies and relatively high mobilities at $T=77^\circ\text{K}$, produces v_d/v_{rms} values between 0.4 and 0.6 in the range 400 to 2000 V/cm.³⁵ Thus the hot carrier distribution is strongly displaced from $k=0$ in the direction of the field. It is indicative of a strong element of streaming motion for the hot carriers. Further development of the streaming picture and its consequences are left for Sec. VIII.

7.5. Energy Gain and Loss Rate of Hot Carriers

In this section, the energy loss rates to optical and acoustical phonons are calculated for the experimentally determined carrier distributions. It is found that the net energy loss rate to optical phonons is dominant and in reasonable quantitative agreement with the directly measured quantity.

For optical phonon interactions, the average power loss per carrier can be given by

$$\left(\frac{d\epsilon}{dt}\right)_{\text{loss}} = \frac{\int_0^{\infty} [\delta\epsilon/(\tau_{\text{opt}e}) - \delta\epsilon/(\tau_{\text{opt}a})] p_E(\epsilon) d\epsilon}{\int_0^{\infty} p_E(\epsilon) d\epsilon} \quad (10)$$

The term in brackets is the difference between the

³⁵ The average energy and v_{rms} pertain to the heavy holes only. The mobility and v_d are determined by both the heavy and light holes. The latter contribute about 30% to the mobility in the Ohmic range, but this percentage is not necessarily sustained at high field. We merely note here that for the heavy holes, v_d/v_{rms} is probably slightly smaller than the values indicated above. The displacement of the light hole distribution is discussed in Sec. VIII.

energy loss and gain rate for a carrier at a given energy due to phonon emission and absorption processes respectively. This term is averaged over the experimentally determined distribution $p_E(\epsilon)$. The energy gained or lost by a hole in a collision $\delta\epsilon$ is that of an optical phonon, $k\theta_{opt}=0.037$ eV. It is independent of the scattering angle, since the optical phonon energy is essentially independent of the phonon wave vector near $k=0$. The collision frequencies for optical phonon emission and absorption processes respectively are taken to be

$$(1/\tau_{opt})_e = (1/\tau_{ac})(\xi_{opt}^2/\xi_{ac}^2)(\theta_{opt}/2T) \times (n+1)(1-k\theta_{opt}/\epsilon)^{1/2}, \quad (11)$$

$$(1/\tau_{opt})_a = (1/\tau_{ac})(\xi_{opt}^2/\xi_{ac}^2)(\theta_{opt}/2T) \times n(1+k\theta_{opt}/\epsilon)^{1/2}, \quad (12)$$

where the phonon occupation number is $n = (e^{\theta_{opt}/T} - 1)^{-1}$, $\theta_{opt} = 430^\circ\text{K}$; ξ_{opt}^2 and ξ_{ac}^2 are coupling constants for optical and acoustical mode scattering, respectively, and τ_{ac} is the relaxation time for acoustical phonon scattering, in terms of which the optical phonon parameters have been expressed following previous practice and notation.¹⁴ The emission can of course only occur for $\epsilon \geq k\theta_{opt}$, while the absorption can occur at all energies. The numerical values used in the above equations are $(\xi_{opt}^2/\xi_{ac}^2) = 3.8$, and $\tau_{ac} = 6.92 \times 10^{-9}/T(\epsilon/k)^{1/2}$ sec. These were previously obtained³⁶ from fitting the temperature dependence of the Ohmic mobility in *p*-type germanium between 20 and 300°K.

For calculating the power loss to acoustical modes, an average of $\delta\epsilon$ over scattering angle must first be taken, since the energy of the acoustical phonon partaking in a collision is a function of the scattering angle. An appropriate expression including emission and absorption was derived by Shockley³⁷; it has only to be divided by τ_{ac} and averaged over the experimental energy distribution.

The calculated energy-loss rates to acoustical and optical phonons as a function of \mathbf{E} , at $T=77^\circ\text{K}$, are separately plotted in Fig. 16. The loss rate to optical phonons is two orders of magnitude larger than to the acoustical phonons. It may be noted that the loss rates were calculated both for $\mathbf{E} \parallel [111]$ and $\mathbf{E} \parallel [100]$; the results are nearly identical even though somewhat different distribution functions had been obtained for these two cases.

The calculated energy loss rates³⁸ can be compared to

³⁶ See Table I in Ref. 14. In this table, the energy ϵ is to be taken in units of °K. Equation (2) in the paper should read $\tau_{ac} = (AT\epsilon^{1/2})^{-1}$. The analysis and approximations under which these values were obtained are discussed in this reference.

³⁷ W. Shockley, Bell. Sys. Tech. J. 30, 990 (1951).

³⁸ We note here some additional implicit assumptions in the determination of the energy-loss rates in the above discussion. It was assumed that the collision time is independent of the direction of the carrier momentum, and hence independent of any anisotropy in the distribution of carriers on any energy surface. Another assumption—valid only for isotropic scattering—is that the collision time can be equated to the current relaxation time which is the quantity actually given by the analysis of the Ohmic mobility (Ref. 14). The degree of validity of these assumptions

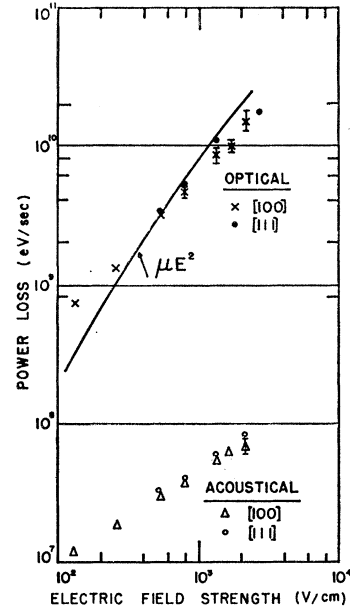


FIG. 16. Field dependence of power loss per carrier for acoustical and optical phonon interactions. The points represent calculations based on experimental distribution functions and previously determined collision frequencies. The solid line is the energy gain rate per carrier, equal in steady state to the energy loss rate, as determined from the measured field dependence of the total hole mobility.

directly measured values. To obtain the latter, we note that the power gain per carrier is equal in steady state to the energy loss rate, and is simply given by μE^2 eV/sec, where μ is the measured, field-dependent mobility. This measured loss rate is represented by the solid line in Fig. 16. The calculated loss rates for optical phonon interactions are in reasonably good agreement with the measured values. The agreement is best at intermediate field strengths, $E \approx 800$ V/cm. It is not surprising that discrepancies should occur at much higher fields, where a large fraction of the power loss is contributed by carriers with energies ≥ 0.06 eV, for which the distribution function has been obtained by extrapolation. At the low-field strengths, part of the discrepancy may be due to the fact that the net energy-loss rate is the difference between roughly comparable loss and gain rates. The latter part depends also on extrapolations of the distribution function at $\epsilon \leq 0.015$ eV.

VIII. MODEL OF STREAMING MOTION: SIGNIFICANCE, RELATION TO SCATTERING MECHANISMS, AND CONSEQUENCES

Common to most theoretical formulations of the hot-carrier effect is the diffusion approximation, in which the

can hardly alter the conclusion that the relative energy-loss rate to acoustical phonons is negligible. For optical phonons, irrespective of the scattering angle, the energy change is very large, and most of the carrier momentum must be lost in any emission process. Thus even for nonisotropic scattering, the collision and relaxation times must be comparable.

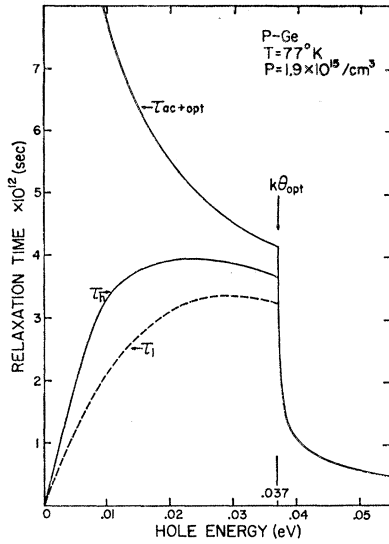


FIG. 17. Relaxation times of heavy (τ_h) and light (τ_l) holes shown as a function of hole energy. The upper curve labeled τ_{ac+opt} is for pure lattice scattering, for which case τ_h is assumed equal to τ_l . The two lower curves incorporate ionized impurity scattering, along with the lattice scattering. The onset of optical phonon emission causes the large drop in relaxation time at energies above 0.037 eV. The values of the relaxation time are calculated on the basis of a previous analysis of the temperature dependence of the zero-field mobility (Ref. 14).

random motion of the carriers is assumed to be strongly predominant over the drift motion even in strong electric field, i.e., the ratio of drift to rms velocity, $v_d/v_{rms} \ll 1$. In this approximation, it is sufficient to retain only the P_0 and P_1 terms in the expansion of the distribution in Legendre polynomials. This approximation should apply when the energy change of the carriers in a collision or between collisions is small compared to the average energy in the steady-state condition. Thus, if the carriers undergo many collisions in transport from one energy to another, this should tend to keep the momentum distribution function nearly isotropic around zero momentum. Accordingly, the diffusion approximation should apply when the scattering is nearly elastic,³⁹ as is the case for acoustical phonon interactions. For the approximation to apply in the case when optical phonon scattering is predominant, it would be necessary that the carriers be very hot, with average energy much greater than the optical phonon energy.

We have already determined that in *p*-type germanium the average energy of the carriers is much less than the optical phonon energy, due to the strength of the optical phonon interaction. We may expect the diffusion approximation not to be applicable here. This is borne out by the magnitude obtained for the ratio v_d/v_{rms} . In this section we will be mainly concerned with presenting a picture of the hot-carrier effect which relates the large values of v_d/v_{rms} to the specific scatter-

³⁹See e.g., S. Chapman and T. G. Cowling, *The Mathematical Theory of Non-Uniform Gases* (Cambridge University Press, Cambridge, 1958), p. 357.

ing mechanisms prevalent in *p*-type germanium. Finally, several interesting consequences of this picture emerge.

It is useful to avail ourselves of the quantitative description of the scattering mechanisms in *p*-type Ge, obtained by Brown and Bray¹⁴ from the analysis of the dependence of the mobility on lattice temperature. We examine in Fig. 17 the variation of hole relaxation time with energy for the combination of ionized impurity, acoustical and optical phonon scattering calculated for a sample with 1.9×10^{15} ionized impurities at $T = 77^\circ\text{K}$. The uppermost curve, for pure lattice scattering, is labeled τ_{ac+opt} , and is assumed to be the same for both light and heavy holes. The inclusion of ionized impurity scattering¹⁴ separates the curves for light and heavy holes (labeled τ_l and τ_h , respectively) and gives the decrease in τ , particularly at low energies. The sharp drop at $\epsilon > 0.037$ eV is due to the strong onset of optical phonon emission processes. For $\epsilon < 0.037$ eV, the dominant contribution to lattice scattering is from acoustical phonon interactions; only a slight decrease in τ , due to scattering by optical phonon absorption, is possible at the low lattice temperature of 77°K . The effects of the very strong optical phonon emission interaction are to provide the high-energy loss rate of the hot holes, and to contain the bulk of the carriers in the energy range $\epsilon < 0.037$ eV.

We may now examine the details of the motion of the carriers when a high field is applied. In the lower energy range, $\epsilon < 0.037$ eV, τ is very large. Hence carriers can accelerate through this entire range with very few collisions, and there is little opportunity for the carrier momentum to be randomized. To illustrate, we note that for a heavy hole, the energy gain in a time $\tau \approx 4 \times 10^{-12}$ sec and for $\mathbf{E} = 500$ V/cm is $(e\mathbf{E}\tau)^2/2m_1^* \approx 0.01$ eV, and increases as \mathbf{E}^2 . For light holes, given such a free time between collisions, the energy gain would be nearly 8 times as large. Thus the carriers acquire a strong element of streaming motion. They are swept into the energy range $\epsilon > 0.037$ eV, where the probability is very high of emitting an optical phonon and returning to low energy. The steady-state situation consists of this cyclic streaming motion⁴⁰ in k space, in sharp contrast to the diffusion picture. The very slow increase in v_d/v_{rms} at $\mathbf{E} > 500$ V/cm suggests that at this field the carriers are already being swept through the low-energy range without being effectively scattered. The main effects of higher fields thereafter are (1) to

⁴⁰A similar picture was originally contemplated by Shockley (Ref. 37) as a limiting high-field effect, in the simple approximation that a carrier attaining the optical phonon emission threshold be instantaneously returned to zero energy. In that case, a saturation in drift velocity should be obtained. In our present case, it is clear that with increasing \mathbf{E} , the penetration of an ever increasing part of the distribution through the emission barrier, must give a slow increase in drift velocity with field strength. A mathematical formulation of the penetration effect and the slow increase in drift velocity has been given by Gunn (Ref. 6, p. 218) for a highly simplified model. The limiting case of Shockley or even of Gunn cannot be applied indiscriminately; it should be quite inadequate when the optical phonon scattering is relatively weak, as e.g., in *n*-type Ge.

increase the frequency of the cyclic streaming, and (2) to enhance the penetration of holes past the optical phonon emission barrier. The average drift velocity and the average energy can not be influenced by the first effect, but both must increase slowly due to the second effect.

The large ratios obtained for v_d/v_{rms} are a consequence of the efficiency of the optical phonon emission interaction which prevents the carriers from becoming really hot, and the weak acoustical phonon interaction which permits the retention of relatively high mobility for the carriers in the energy range to which they are constrained. To emphasize the important role of the strong optical phonon interaction, we may consider what would happen if it were not present. Upon application of the field, the carriers would initially still stream through the low-energy range, but with no optical phonon emission barrier to stop them, they would continue on to very high energies, where eventually the acoustical scattering mechanism would become strong enough (since $\tau_{ac} \propto \epsilon^{-1/2}$) to enforce a steady-state distribution. In this situation the average energy of the carriers would be very high; with τ_{ac} being much smaller at high energies, the ratio of v_d/v_{rms} would be $\ll 1$, and the diffusion approximation would be applicable. We note that in *n*-type germanium, the optical phonon interaction is an order of magnitude weaker than in *p*-type germanium.¹³ Consequently we may expect that in the former case much higher energies would be attained. The noise measurements of Erlbach and Gunn⁷ on *n*-type germanium do indeed indicate very much higher effective electron temperatures than we obtain in the present experiment for holes. It is also significant that the hot-carrier mobility theory formulated in the diffusion approximation gives much better fit to experiment in *n*-type than in *p*-type germanium.⁴¹ A hot carrier mobility theory based on the picture of cyclic streaming motion remains to be developed.

The consequences of the present picture are particularly interesting for the case of the light holes. The streaming effect must become important for them at much lower fields than for the heavy holes. The light holes, being accelerated to the optical phonon emission threshold much more rapidly than heavy holes, must undergo optical phonon emission much more frequently. Since they are presumed to be predominantly scattered into the heavy hole band, there must be a depopulation of the light hole band with increasing field strength.⁴² This should contribute appreciably to a decrease in total hole mobility even at relatively low-field strengths. The assumption was made in past analyses of hot-carrier mobility in *p*-type germanium that the temperature was the same for both heavy and light holes, and that there

was no redistribution in populations.^{13,15} In a diffusion approximation, such assumptions would be very reasonable. If the relative strength of inter- or intravalence-band scattering is determined purely by the density of final states available, then any hole can be expected to spend only about 4% of its time as a light hole. With the provision that energy gain in any mean free time is small compared to average energy, then the average energy of heavy or light holes is determined over many mean free times, most of which have been spent as heavy holes. Thus the history must be the same for all carriers, irrespective of whether they are instantaneously light or heavy, and hence their temperatures or average energies must be the same. In this case the populations must be determined only by the relative density of states, and should not change with field, provided the carriers remain at energies where the effective masses are constant.

Several other consequences of the picture of the hot-carrier effect in *p*-type germanium will be briefly described now, but the detailed analysis and experimental evidence will be presented elsewhere.

a. Anisotropic Infrared Absorption

If the carrier distribution is strongly displaced in *k* space, it is obvious that the angular distribution of the carriers on surfaces of constant energy must become highly anisotropic and that higher order terms than P_0 and P_1 in the expansion of the distribution function must be taken into account. This leads to the expectation that the intervalence band absorption should become dependent on the direction of polarization of the infrared radiation relative to the field direction. As already noted in Sec. 3.3c, this effect has been observed and analyzed elsewhere.^{4,5}

b. Anisotropy of Hot-Carrier Mobility

The Ohmic mobility is isotropic in *p*-type germanium, in spite of the warped energy surfaces, because of cubic symmetry. For hot carriers, the streaming motion prevents the carriers from experiencing the full crystal symmetry, and consequently the mobility should become dependent on the crystallographic orientation of the field.⁴³ An anisotropy of the mobility has been observed²⁷; the mobility at high field is highest for the [100], smaller for the [110], and least for the [111] orientation. However, the differences are not very large, of the order of 15% between the [100] and [111] directions.²⁷ The above order of the high-field mobilities is qualitatively consistent with the reverse order of the effective mass ratios ($m_{<100>}^* = 0.28$, $m_{<110>}^* = 0.35$, and $m_{<111>}^* = 0.37$).

c. Impact Ionization of Acceptors

The curtailment of hot carriers at energies above 0.037 eV due to the strength of the optical phonon emis-

⁴¹ For evidence of the fit of the theory to *n*-type Ge, see H. G. Reik and H. Risken, Phys. Rev. **126**, 1737 (1962); also compare results for *p* and *n*-type Ge in Ref. 13.

⁴² The only experimental evidence available to support this point is the rather speculative conclusion derived from the effective temperature analysis in Sec. V.

⁴³ This has already been pointed out by Baynham and Paige (Ref. 5).

sion process should manifest itself in the inefficiency of impact ionization of acceptor impurities with large ionization energies.⁴⁴ In confirmation, it has been found to be very difficult to achieve appreciable ionization of Cu and Zn acceptors, having ionization energies of 0.043 and 0.033 eV, respectively.⁴⁵

IX. SUMMARY AND CONCLUSIONS

The modulation of the intervalence band absorption of infrared radiation by pulses of hot carriers has been studied. The modulation effects are of interest for their own sake; nearly 50% positive and negative modulation was obtained at certain wavelengths at $E \leq 2800$ V/cm. A minor dependence of the modulation on the crystallographic direction of the electric field was observed. No dependence was observed on carrier concentration in the range 0.6 to $1.9 \times 10^{15}/\text{cm}^3$ within experimental error. There is a major dependence of the modulation on the direction of polarization of light relative to the field direction.

The main objective was to determine the energy distribution functions of the hot carriers. The analysis was based on a combination of (a) a theoretical description of the basic absorption processes in terms of direct or vertical transitions of carriers between the various valence bands, and (b) an empirical determination of the necessary quantitative details, such as the shape of the valence bands, and the relationship between absorption coefficient and hole concentration. The empirical information was obtained from an auxiliary study of the temperature dependence of the equilibrium absorption spectrum. This yielded an approximate valence band structure, with equivalent spherical energy surfaces, to represent the actual, more complicated band structure. It was feasible to apply this empirical model only for the study of the heavy hole distribution. Because of the approximations, the energy distribution functions were obtained with limited resolution. Nevertheless, many valuable details were obtained. The main results may be summarized as follows:

(1) The hot-carrier distribution functions are non-Maxwellian, and typified by the relatively small number

of carriers in the high-energy tail of the distribution at $\epsilon > 0.037$ eV, the optical phonon emission threshold.

(2) The average energy of the carriers increases only very slowly with field strength, indicating the existence of strong energy-loss processes.

(3) The ratio of drift to root-mean-square velocity, determined from mobility measurements and the average energy, becomes very large, $v_d/v_{\text{rms}} \geq 0.4$ at $E \geq 400$ V/cm, corresponding to strong displacement of the distribution in momentum space. A strong anisotropy in the distribution of holes on surfaces of constant energy is deduced.

These three features were shown to be consistent with a description of the scattering processes previously deduced from the temperature dependence of the Ohmic mobility. The strong inelastic scattering could be attributed to the high rate of emission of optical phonons by carriers with $\epsilon \geq 0.037$ eV. This has the effect of containing a major fraction of the carriers in the energy range $\epsilon \leq 0.037$ eV, in which the collision time, determined primarily by acoustical phonon and ionized impurity scattering, is relatively long. The calculated energy loss rate to optical phonons, using the experimental distribution functions, was found to be in good agreement with the directly measured energy loss rate μE^2 . Thus the strength of the optical phonon interaction, previously determined empirically from the temperature dependence of the ohmic mobility, enabled us here to quantitatively account for the energy loss rate of the hot carriers, without further adjustment of parameters. A picture of the steady state hot carrier effect emerged which emphasized the cyclic streaming motion of the carriers in \mathbf{k} space. The carriers stream with few collisions to energies > 0.037 eV and then return to low energies to repeat the process. A possible depletion in light-hole population at high fields is deduced.

The insight afforded into the nature of the distribution functions of the hot carriers suggest that in p -type germanium the streaming rather than the heating aspect of the "hot" carriers should be given strong emphasis in interpreting such transport properties as the field dependence of the mobility, and hot carrier mobility anisotropy.

ACKNOWLEDGMENTS

We are indebted to A. K. Ramdas and P. Fisher for advice and assistance in the use of infrared equipment, and particularly to R. L. Petritz of Texas Instruments, Inc., for the use of the InSb detector.

⁴⁴ Such an effect was predicted by M. Lampert, F. Herman, and M. C. Steele, *Phys. Rev. Letters* **2**, 394 (1959), who did not however consider quantitatively how strong the optical phonon interaction had to be to obtain such a result.

⁴⁵ D. M. Brown and R. Bray, *Bull. Am. Phys. Soc.* **6**, 139 (1961).